JOC The Journal of Organic Chemistry

Article

pubs.acs.org/joc

Control of Regioselectivity and Stereoselectivity in (4 + 3) Cycloadditions of Chiral Oxyallyls with Unsymmetrically Disubstituted Furans

Yunfei Du,[†] Elizabeth H. Krenske,*[,‡] Jennifer E. Antoline,[§] Andrew G. Lohse,[§] K. N. Houk,*[,∥] and Richard P. Hsung*[,§]

[†]School of Pharmaceutical Science and Technology, Tianjin University, Tianjin, 300072, P. R. China

[‡]School of Chemistry, University of Melbourne, Victoria 3010, Australia and Australian Research Council Centre of Excellence for Free Radical Chemistry and Biotechnology

[§]Division of Pharmaceutical Sciences and Department of Chemistry, University of Wisconsin at Madison, Madison, Wisconsin 53705, United States

[∥]Department of Chemistry and Biochemistry, University of California, Los Angeles, California 90095, United States

Supporting Information

ABSTRACT: The regioselectivities and stereoselectivities of $ZnCl_2$-catalyzed (4 + 3) cycloadditions between chiral oxazolidinone-substituted oxyallyls and unsymmetrical disubstituted furans have been determined. The substitution pattern on the furan is found to provide a valuable tool for controlling the stereochemistry (*endo-I* or *endo-II*) of the 7-membered cycloadduct. While cycloadditions with monosubstituted furans usually favor *endo-I* products, from addition of the furan to the more crowded face of the oxyallyl, cycloadditions with 2,3- and 2,5-disubstituted furans instead favor the *endo-II* stereochemistry. Density functional theory calculations are performed to account for the selectivities. For monosubstituted furans, the crowded transition state leading to the *endo-I* cycloadduct is stabilized by an edge-to-face interaction between the furan and the oxazolidinone 4-Ph group, but this stabilization is overcome by steric clashing if the furan bears a 2-CO_2R group or is 2,3-disubstituted.

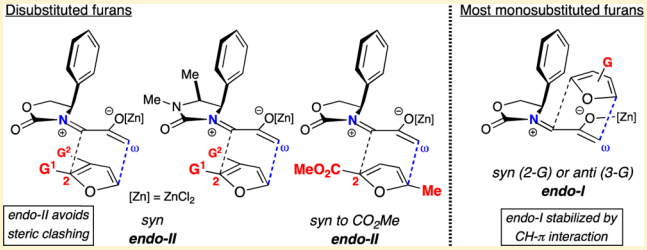

INTRODUCTION

Oxazolidinone-stabilized oxyallyls (**3**) are a fascinating class of reactive intermediates, generated by oxidation of allenamides (**1**).[1,2] Several valuable synthetic routes to 7-membered carbocycles rely on (4 + 3) cycloadditions between oxyallyl intermediates and dienes,[3,4] and we have found that the cycloadditions of oxyallyls **3** with monosubstituted furans (Schemes 1 and 2) display distinctive regioselectivities and stereoselectivities.[5,6] These reactions may be performed either under thermal conditions or with catalysis by $ZnCl_2$. The regioselectivities are summarized in Scheme 1, which shows the achiral oxyallyl **3a**; cycloadditions of **3a** with 2-substituted furans (G = Me or CO_2Me) favor the "*syn*" regiochemistry, while reactions with 3-substituted furans favor "*anti*" regiochemistry. The same regioselectivities are obtained with the chiral oxyallyl **3b** (Scheme 2), but in this case the reactions also feature a novel mode of stereoinduction. Surprisingly, reactions of **3b** with most monosubstituted furans were found to favor the *endo-I* stereochemistry, which entails addition of the furan to the more crowded face of **3b**. Density functional theory calculations[6] showed that the crowded transition state is favored because it contains a stabilizing edge-to-face aromatic interaction (CH−π) between furan and Ph. Of the monosubstituted furans studied, only those containing a 2-CO_2R group did not follow this behavior.

In order to explore the generality of these stereochemical and regiochemical control elements, we have examined the (4 + 3) cycloadditions of **3b** with more complex, unsymmetrical disubstituted furans. We report that these reactions often proceed with high levels of regio- and stereocontrol, even when the selectivities cannot be easily predicted from individual substituent effects. Complete control over stereoselectivity can be obtained through strategic choice of substituents.

RESULTS AND DISCUSSION

We investigated the (4 + 3) cycloadditions of oxyallyls **3** with a range of unsymmetrical disubstituted furans containing Me and CO_2Me substituents at different positions. The cycloadditions were performed under $ZnCl_2$-catalyzed conditions. Results are given in Table 1.

Our work commenced with the 2-CO_2Me,3-Me-substituted furan, **4**. Based on the selectivities previously observed with

Special Issue: Howard Zimmerman Memorial Issue

Received: June 7, 2012
Published: July 31, 2012

   dx.doi.org/10.1021/jo3011792 | J. Org. Chem. 2013, 78, 1753−1759

Scheme 1. Regioselectivities of (4 + 3) Cycloadditions of Achiral Oxyallyl 3a with Monosubstituted Furans[6b]

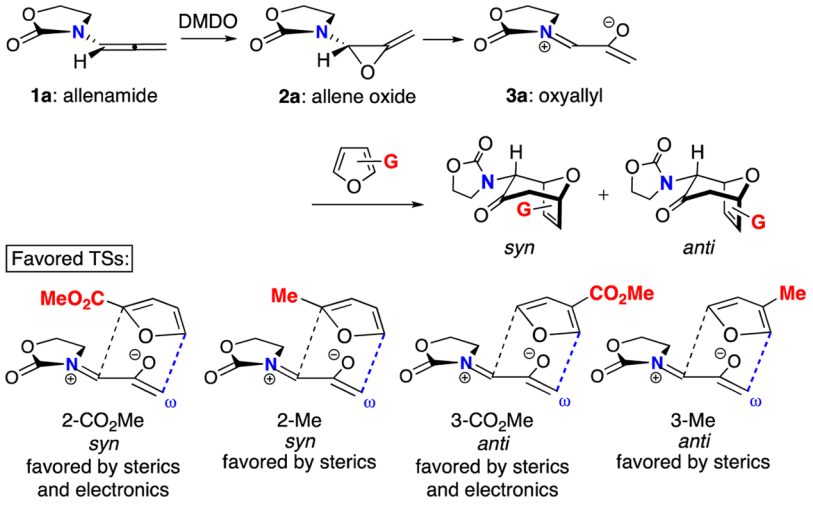

Scheme 2. Stereoselectivities of (4 + 3) Cycloadditions of Chiral Oxyallyl 3b with Monosubstituted Furans[6a,c]

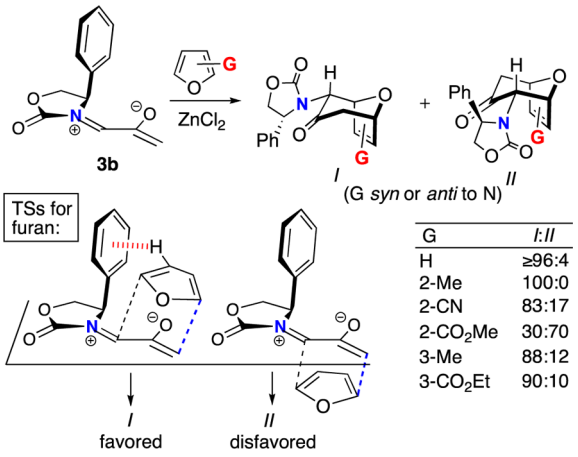

G	I:II
H	≥96:4
2-Me	100:0
2-CN	83:17
2-CO_2Me	30:70
3-Me	88:12
3-CO_2Et	90:10

monosubstituted furans (Schemes 1 and 2), it is not possible to predict the major product for **4**; a 2-CO_2Me substituent favors *syn-II* but a 3-Me substituent favors *anti-I*. The cycloaddition of **3b** with **4** was found to give exclusively the *syn-II* cycloadduct, **8**, in 67% yield. The structure of **8** was assigned unambiguously by X-ray (Figure 1). The cycloaddition of **3b** with the 2-Me,3-CO_2Me-substituted furan **5** also gave exclusively a *syn-II* adduct (**9**). Confirmation of the structure of **9** was obtained following reduction/esterification, which afforded a rearranged derivative (**12**) whose X-ray structure was determined (Figure 1).[7] The regioselectivities observed for both **4** and **5** match those previously obtained[6b] with the achiral oxyallyl **3a**, which displayed *syn* selectivities of ≥95:5.

We next examined the 2-Me,3-Me-substituted furan, **6**. In order to deal with competing oxidation of this more electron-rich furan, we had to switch to the more reactive allenamide, **1c**,[8] which contains Close's chiral imidazolidinone auxiliary.[9] Previous experiments[5] indicated that Close's imidazolidinone controls stereoselectivity in the same way as 4-Ph-oxazolidinone. Cycloaddition of **3c** with **6** afforded mainly the *syn-II* product, **10c**, but also gave two other cycloadducts: *syn-I* (**10a**) and *anti-I* (**10b**). X-ray structures were determined for the two minor products (Figure 1), while the major product was assigned unambiguously by NOESY and COSY (see the Supporting Information).

In 2,3-disubstituted furans, the substituents have opposite regiodirecting influences (Scheme 1), and the selectivities obtained with **4**–**6** indicate that it is the 2-substituent that dictates the outcome. In order to discern the relative directing power of Me and CO_2Me groups at the 2-position, we examined the reaction of **3b** with **7**. The only cycloadduct detected was **11**, where CO_2Me is *syn* to nitrogen. Its structure was confirmed by NOESY and COSY.

The regioselectivities and stereoselectivities observed here with disubstituted furans are quite distinct from those reported previously for monosubstituted furans.[6] We performed density functional theory calculations to explore the selectivities. Transition states for $ZnCl_2$-catalyzed cycloadditions of the oxyallyls **3b** and **3c** with furans **4**–**7** were computed at the B3LYP/6-31G(d) level (with LANL2DZ on Zn), as we have previously done in our studies of related oxyallyl (4 + 3) cycloadditions. The transition states for the reaction of **3b** with **4** are representative and are shown in Figure 2. Regardless of the regiochemistry, the transition states each show the same sense of asynchronicity, with more advanced bonding at the unsubstituted terminus of the oxyallyl. The HOMO coefficient of the oxyallyl is larger at this terminus.

We previously found that B3LYP activation energies provide good predictions of regioselectivity and stereoselectivity for oxyallyl (4 + 3) cycloadditions. In order to provide a better treatment of dispersion energies in the cycloadditions of **4**–**7**, which are likely to vary significantly between stereoisomeric transition states *I* and *II*, we calculated the activation barriers from single-point energies at the M06-2X/6-311+G(d,p) level. Solvent effects were modeled by means of CPCM calculations. The M06-2X activation energies in the gas phase and in dichloromethane are given in Table 2.

The calculated values of $\Delta G^{\ddagger}$ in the gas phase and in solution predict a strong preference for the observed product (*syn-II*) for both furans **4** and **5**. The *syn-II* TS from **4** is favored by ≥2.9 kcal/mol in dichloromethane, and the *syn-II* TS from **5** is favored by ≥4.6 kcal/mol. Lower selectivity is predicted for furan **6**. Indeed, the cycloaddition of **6** with **3b** is calculated to favor the *anti-I* TS by 0.6 kcal/mol. However, the cycloaddition of the same furan with **3c**, which was studied experimentally, is correctly predicted to favor *syn-II*. The *syn-II* TS is preferred by

dx.doi.org/10.1021/jo3011792 | J. Org. Chem. 2013, 78, 1753–1759

Table 1. (4 + 3) Cycloadditions of Oxyallyls with Disubstituted Furans[a]

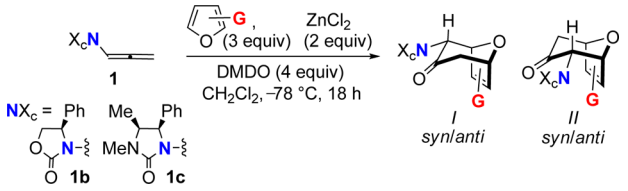

furan	*syn-I*	*anti-I*	*syn-II*	*anti-II*	yield (%)
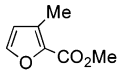 **4**	–	–	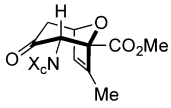 **8** (100)	–	67[b]
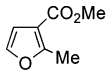 **5**	–	–	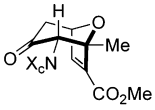 **9** (100)	–	60[b]
 **6**	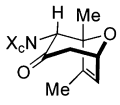 **10a** (15)	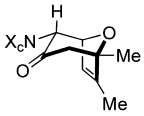 **10b** (35)	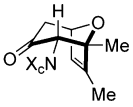 **10c** (50)	–	61[c]
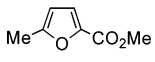 **7**	–	–	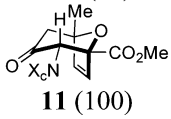 **11** (100)	–	40[b]

[a]Isolated yields are quoted. Isomer ratios are given in parentheses and were determined by ^{1}H and/or ^{13}C NMR. [b]From reaction with allenamide **1b**. [c]From reaction with allenamide **1c**.

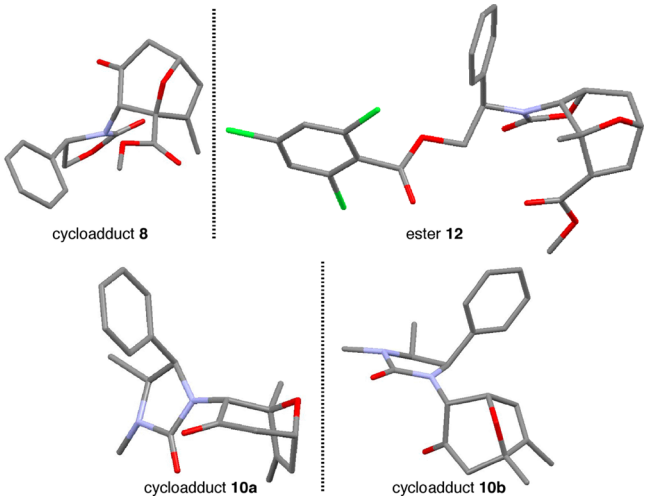

Figure 1. X-ray structures of cycloadduct **8**, ester **12** (derived from **9**), and cycloadducts **10a** and **10b**.

0.1–0.2 kcal/mol over *syn-I* and *anti-I*. Experimentally, a mixture of products was obtained containing the latter two isomers as minor products. The agreement between experiment and theory is not as good for **7**, where the calculations predict a 1.1 kcal/mol preference for *anti-I* in dichloromethane. The selectivity in the gas phase does correctly predict *syn-II*, however. Experimentally, the *syn-II* cycloadduct was obtained in 40% yield.

Activation energies were also computed with a second dispersion-inclusive functional, B3LYP-D3 (Supporting Information). The predicted selectivities mirror those from M06-2X. B3LYP alone also correctly predicts the major products for furans **4**–**6** (and from **7** in the gas phase), but fails to predict the presence of minor products in the cycloaddition involving **6**.

Our previous calculations showed that a 2-substituent on the furan favors *syn* regiochemistry because the shorter forming bond in the transition state is located at the less-hindered carbon (C-5) of the furan.[6] When the 2-substituent is electron-withdrawing, this steric effect is reinforced by a strong oxyallyl–furan interaction energy, related to the large furan LUMO coefficient at C-5. For 3-substituted furans, by contrast, the *anti* regiochemistry is favored because its transition state avoids steric clashing between the 3-substituent and the oxazolidinone.

The *syn* selectivities obtained experimentally from furans **4**–**7** (Table 1) indicate that the regiodirecting influence of a 2-substituent outweighs that of a 3-substituent, regardless of whether the substituent is Me or CO_2Me. A 2-CO_2Me group exerts a stronger regiodirecting effect than a 2-Me group (cf. **7**) because the oxyallyl–furan interaction in the TS is stronger when CO_2Me is *syn* to nitrogen.

The stereoselectivities observed with furans **4**–**7** cannot be predicted from those of the corresponding monosubstituted furans. Most monosubstituted furans favor diastereomer *I*, due to the stabilizing edge-to-face aryl–aryl interaction in the crowded (*I*) transition state (Scheme 2).[6a,c] Only for 2-CO_2Me-furan was *II* favored; in that case, the (*syn*-)*I* TS is destabilized by electrostatic repulsion between the CO_2Me group and the Ph π-cloud.

A similar type of repulsive electrostatic effect influences the stereoselectivities for **4** and **7**, favoring *II*. More generally, however, the stereoselectivities for all three 2,3-disubstituted furans (**4**–**6**) are dictated by the furan 3-substituent. This

dx.doi.org/10.1021/jo3011792 | J. Org. Chem. 2013, 78, 1753–1759

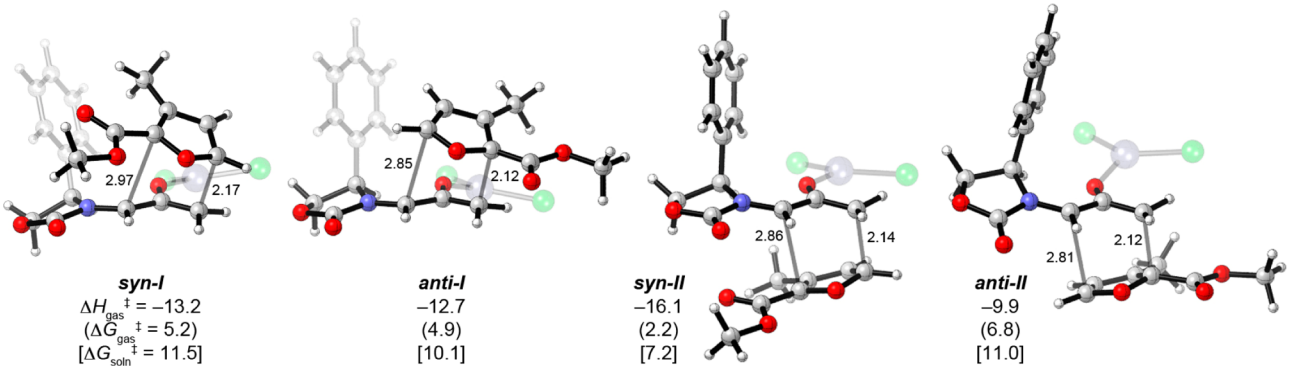

Figure 2. Transition structures for $ZnCl_2$-catalyzed cycloadditions of oxyallyl **3b** with furan **4**, optimized with B3LYP. Below each structure are given the activation energies obtained from M06-2X single-point calculations. Distances in Å, $\Delta H^{\ddagger}$ and $\Delta G^{\ddagger}$ in kcal/mol.

Table 2. Calculated Activation Energies for $ZnCl_2$-Catalyzed Cycloadditions of 3b with Disubstituted Furans[a]

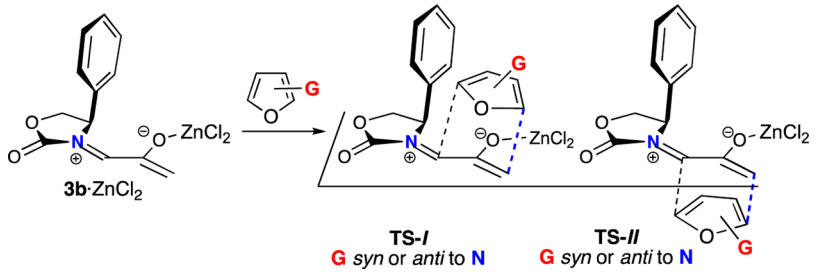

	$\Delta H^{\ddagger}$ ($\Delta G^{\ddagger}$) [$\Delta G^{\ddagger}_{soln}$]			
reactants	*syn-I*	*anti-I*	*syn-II*	*anti-II*
4 + **3b**·$ZnCl_2$	−13.2	−12.7	−16.1	−9.9
	(5.2)	(4.9)	(2.2)	(6.8)
	[11.5]	[10.1]	[7.2]	[11.0]
5 + **3b**·$ZnCl_2$	−13.2	−15.5	−14.6	−13.0
	(4.3)	(3.6)	(2.6)	(5.6)
	[12.5]	[11.9]	[7.3]	[14.1]
6 + **3b**·$ZnCl_2$	−12.8	−15.0	−12.1	−12.4
	(3.9)	(2.3)	(3.6)	(3.9)
	[8.4]	[7.4]	[8.0]	[8.0]
6 + **3c**·$ZnCl_2$	−7.0	−8.3	−6.1	−6.0
	(9.7)	(9.0)	(9.6)	(10.4)
	[14.3]	[14.4]	[14.2]	[14.9]
7 + **3b**·$ZnCl_2$	−9.6	−11.5	−14.4	−8.3
	(8.4)	(4.8)	(3.8)	(7.0)
	[16.1]	[9.9]	[11.0]	[11.4]

[a]M06-2X/6-311+G(d,p)//B3LYP/6-31G(d)-LANL2DZ. Solution-phase data incorporate CPCM solvation energies in CH_2Cl_2, computed at the M06-2X/6-31G(d)-LANL2DZ level. $\Delta H^{\ddagger}$ and $\Delta G^{\ddagger}$ in kcal/mol at 298.15 K.

group eliminates the possibility of an edge-to-face CH−π interaction in the crowded *syn-I* TS and replaces it with a repulsive electrostatic interaction (3-CO_2Me) or a weaker CH−π interaction (3-Me). The result is a preference for *II*. Only for **6**, where no CO_2Me group is present, are isomers of *I* found as minor products.

CONCLUSION

The investigations detailed herein provide a valuable new approach to controlling the stereoselectivities of (4 + 3) cycloadditions. The different classes of substituent effects operating for monosubstituted and disubstituted furans are outlined in Scheme 3 and can be summarized as follows: cycloaddition of oxyallyl **3b** or **3c** with a 2-substituted furan (including a disubstituted furan) favors the *syn-I* cycloadduct, unless (a) the 2-substituent is CO_2R or (b) there is also a substituent present at furan C-3. In the latter two cases, *syn-II* is preferred instead. These principles enable cycloadditions of oxyallyls **3** with complex furans to be achieved with high levels of regioselectivity and stereoselectivity.

EXPERIMENTAL SECTION

General Procedure for Allenamide (4 + 3) Cycloadditions. To a solution of a respective allenamide in CH_2Cl_2 (0.1 M) was added 3−9 equiv of the appropriate furan and 4 Å powdered molecular sieves (0.5 g). The reaction solution was cooled to −78 °C, and 2.0 equiv of $ZnCl_2$ (1.0 M in Et_2O) was added. Dimethyldioxirane (DMDO) (4.0−6.0 equiv) in acetone was then added as a chilled solution (at −78 °C) via a syringe pump over 3−4 h. The syringe pump was cooled using dry ice during the entire addition time. After the addition, the reaction mixture was stirred for an additional 14 h before it was quenched with

dx.doi.org/10.1021/jo3011792 | J. Org. Chem. 2013, 78, 1753−1759

Scheme 3. Summary of Substituent-Controlled Regioselectivity and Stereoselectivity in (4 + 3) Cycloadditions of Oxyallyl 3b with Furans

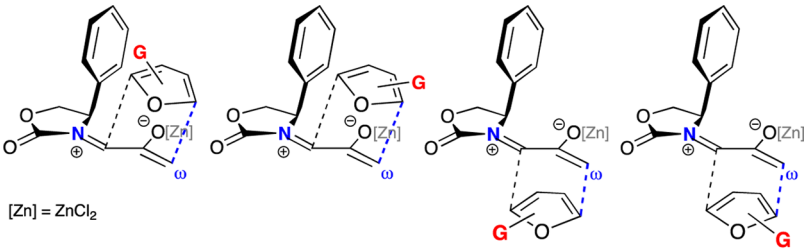

syn-I	*anti-I*	*syn-II*	*anti-II*
Favored for:	Favored for:	Favored for:	Favored for:
2-Me	3-Me	2-CO_2Me	none
2-CN	3-CO_2R	2-CO_2Me,5-Me	
	3-Br	2-CO_2Me,3-Me	
	3-Ph	2-Me,3-CO_2Me	
	3-CH_2OAcyl	2-Me,3-Me	

satd aq $NaHCO_3$, filtered through Celite, concentrated in vacuo, and extracted with CH_2Cl_2 (4 × 20 mL). The combined organic layers were dried over Na_2SO_4 and concentrated in vacuo. The crude residue was purified via silica gel column chromatography (gradient eluent: 10−75% ethyl acetate in hexane).

8: reaction scale, 0.50 mmol of allenamide **1b**; yield 67%; mass 119.6 mg; R_f = 0.13 (50% EtOAc in hexane); $[\alpha]^{23}_D$ −169.6 (*c* 4.6, CH_2Cl_2); white solid; mp = 119−120 °C; ^{1}H NMR (400 MHz, $CDCl_3$) δ 2.04 (s, 3H), 2.54 (d, 1H, *J* = 16.0 Hz), 2.83 (dd, 1H, *J* = 5.4, 16.0 Hz), 3.29 (s, 3H), 3.91 (s, 1H), 4.20 (t, 1H, *J* = 9.0 Hz), 4.62 (t, 1H, *J* = 9.0 Hz), 4.79 (t, 1H, *J* = 9.0 Hz), 4.90 (dt, 1H, *J* = 5.2, 1.6 Hz), 7.00 (d, 1H, *J* = 1.6 Hz), 7.31−7.45 (m, 5H); ^{13}C NMR (100 MHz, $CDCl_3$) δ 15.3, 44.3, 52.6, 65.9, 68.5, 70.5, 76.8, 88.3, 128.7, 129.3, 129.7, 130.2, 136.6, 142.9, 158.5, 166.9, 200.9; IR (thin film) cm^{-1} 3280w, 2911w, 1766s, 1437w; mass spectrum (APCI) *m*/*e* (relative intensity) 358.1 (100) $(M + H)^+$; HRMS (MALDI-TOF): *m*/*e* calcd for $C_{19}H_{19}NO_6Na^+$ $(M + Na^+)$ 380.1105, found 380.1097.

9: reaction scale, 1.00 mmol of allenamide **1b**; yield 60%; mass 214.2 mg; R_f = 0.25 (50% EtOAc in hexane); $[\alpha]^{23}_D$ −74.5 (*c* 4.0, CH_2Cl_2); ^{1}H NMR (500 MHz, $CDCl_3$) δ 1.30 (s, 3H), 2.60 (d, 1H, *J* = 17.5 Hz), 2.88 (dd, 1H, *J* = 6.0, 17.5 Hz), 3.45 (s, 1H), 3.80 (s, 3H), 4.36 (t, 1H, *J* = 9.0 Hz), 4.71 (t, 1H, *J* = 9.0 Hz), 4.83 (t, 1H, *J* = 9.0 Hz), 4.99 (dd, 1H, *J* = 6.0, 2.0 Hz), 7.08 (d, 1H, *J* = 0.25 Hz), 7.48−7.52 (m, 5H); ^{13}C NMR (125 MHz, $CDCl_3$) δ 15.4, 44.3, 52.6, 66.0, 68.6, 70.6, 76.9, 88.4, 126.4, 128.8, 129.4, 129.8, 130.3, 143.0, 158.6, 167.0, 201.0; IR (thin film) cm^{-1} 2954s, 2930s, 1764s, 1726s; mass spectrum (APCI) *m*/*e* (relative intensity) 358.2 (100) $(M + H)^+$; HRMS (MALDI-TOF) *m*/*e* calcd for $C_{19}H_{19}NO_6Na^+$ $(M + Na^+)$ 380.1105, found 380.1095.

10a: reaction scale, 0.44 mmol of allenamide **1c**; yield 9%; mass 13.5 mg; R_f = 0.22 (50% EtOAc in hexane); $[\alpha]^{23}_D$ +14.9 (*c* 0.75, CH_2Cl_2); mp = 162−163 °C; ^{1}H NMR (400 MHz, $CDCl_3$) δ 0.79 (d, 1H, *J* = 6.8 Hz), 1.46 (s, 3H), 1. 81 (s, 3H), 2.49 (d, 1H, *J* = 17.8 Hz), 2.60 (dd, 1H, *J* = 5.8, 17.8 Hz), 2.69 (s, 3H), 3.29 (s, 1H), 3.82 (dq, 1H, *J* = 6.8, 9.2 Hz), 4.70 (d, 1H, *J* = 9.2 Hz), 4.75 (d, 1H, *J* = 5.8 Hz), 5.91 (s, 1H), 7.13 (br, 1H), 7.32 (br, 4H); ^{13}C NMR (100 MHz, $CDCl_3$) δ 14.0, 15.5, 21.4, 29.3, 43.8, 56.6, 65.2, 69.3, 75.9, 86.8, 128.5, 128.8, 128.9, 129.5, 135.3, 144.8, 159.3, 200.9; IR (thin film) cm^{-1} 2929 m, 1725s, 1687s, 1432 m, 1263 m, 1161 m, 736 m, 694s; mass spectrum (APCI) *m*/*e* (relative intensity) 341.2 (60) $(M + H)^+$; HRMS (MALDI-TOF) *m*/*e* calcd for $C_{20}H_{24}N_2O_3Na^+$ $(M + Na^+)$ 363.1679, found 363.1680.

10b: reaction scale, 0.44 mmol of allenamide **1c**; yield 21%; mass 31.4 mg; R_f = 0.17 (50% EtOAc in hexane); $[\alpha]^{23}_D$ −184.3 (*c* 0.79, CH_2Cl_2); white solid; mp = 194−195 °C; ^{1}H NMR (400 MHz, $CDCl_3$) δ 0.71 (d, 1H, *J* = 6.8 Hz), 1.34 (s, 3H), 1.59 (s, 3H), 2.44 (d, 1H, *J* = 15.6 Hz), 2.57 (d, 1H, *J* = 15.6 Hz), 2.73 (s, 3H), 3.96 (dq, 1H, *J* = 6.8, 8.8 Hz), 4.46 (d, 1H, *J* = 8.8 Hz), 4.49 (d, 1H, 4.2 Hz), 4.66 (s, 1H), 5.10 (d, 1H, *J* = 4.2 Hz), 7.03 (br, 1H), 7.31−7.33 (m, 1H); ^{13}C NMR (100 MHz, $CDCl_3$) δ 12.1, 15.3, 21.6, 29.3, 50.8, 57.2, 59.7, 64.5, 79.2, 85.9, 125.6, 127.4, 128.4, 129.2, 138.8, 146.3, 162.6, 203.8; IR (thin film) cm^{-1} 2941 m, 1728s, 1686s, 1431 m, 1255 m, 1196s, 1025 m, 855s, 735s, 700s; mass spectrum (APCI) *m*/*e* (relative intensity) 339.2 (45) $(M-H)^-$; HRMS (MALDI-TOF) *m*/*e* calcd for $C_{20}H_{24}N_2O_3Na^+$ $(M + Na^+)$ 363.1679, found 363.1678.

10c: reaction scale, 0.44 mmol of allenamide **1c**; yield 31%; mass 46.4 mg; R_f = 0.23 (50% EtOAc in hexane); $[\alpha]^{23}_D$ −105.7 (*c* 0.83, CH_2Cl_2); colorless oil; ^{1}H NMR (400 MHz, $CDCl_3$) δ 0.85 (d, 1H, *J* = 6.8 Hz), 1.13 (s, 3H), 1. 89 (s, 3H), 2.47 (d, 1H, *J* = 17.2 Hz), 2.71 (dd, 1H, *J* = 5.8, 17.2 Hz), 2.79 (s, 3H), 3.43 (s, 1H), 3.92 (dq, 1H, *J* = 6.8, 9.2 Hz), 4.61 (d, 1H, *J* = 9.2 Hz), 4.74 (d, 1H, *J* = 5.8 Hz), 5.86 (s, 1H), 7.27−7.34 (m, 5H); ^{13}C NMR (100 MHz, $CDCl_3$) δ 14.4, 15.1, 21.4, 29.1, 44.7, 56.3, 68.1, 74.9, 75.9, 87.7, 121.1, 128.5, 128.8, 129.5, 137.0, 146.9, 161.7, 204.2; IR (thin film) cm^{-1} 2933 m, 1703s, 1431, 1400s, 1262 m, 1159 m, 762 m; mass spectrum (APCI) *m*/*e* (relative intensity) 341.2 (60) $(M + H)^+$; HRMS (MALDI-TOF) *m*/*e* calcd for $C_{20}H_{24}N_2O_3Na^+$ $(M + Na^+)$ 363.1679, found 363.1674.

11: reaction scale, 0.35 mmol of allenamide **1b**; yield 40%; mass 50.0 mg; R_f = 0.22 (50% EtOAc in hexane); $[\alpha]^{23}_D$ −31.4 (*c* 6.4, CH_2Cl_2); ^{1}H NMR (500 MHz, $CDCl_3$) δ 1.43 (s, 3H), 2.59 (d, 1H, *J* = 16.0 Hz), 2.68 (dd, 1H, *J* = 5.2, 16.0 Hz), 3.65 (s, 3H), 3.93 (s, 1H), 4.18 (t, 1H, *J* = 9.0 Hz), 4.65 (t, 1H, *J* = 9.0 Hz), 4.82 (t, 1H, *J* = 9.0 Hz), 6.07 (d, 1H, *J* = 6.0 Hz), 6.66 (d, 1H, *J* = 6.0 Hz), 7.28−7.41 (m, 5H); ^{13}C NMR (100 MHz, $CDCl_3$) δ 23.2, 51.3, 64.4, 67.2, 70.5, 72.8, 86.1, 89.4, 126.4, 128.4, 129.9, 133.4, 135.6, 136.5, 158.1, 167.5, 199.8; IR (thin film) cm^{-1} 3520w, 2957w, 2927w, 1759s, 1726s; mass spectrum (APCI): *m*/*e* (relative intensity) 358.2 (35) $(M + H)^+$; HRMS (MALDI-TOF) *m*/*e* calcd for $C_{19}H_{19}NO_6Na^+$ $(M + Na^+)$ 380.1105, found 380.1090.

Synthesis of Ester 12 from Cycloadduct 9. To a solution of cycloadduct **9** (53.6 mg, 0.150 mmol) in anhyd MeOH (5 mL) was added $NaBH_4$ (34.2 mg, 0.904 mmol) portionwise within 1 h at 0 °C. The reaction mixture was further stirred at room temperature for 6 h until the consumption of the starting material. Saturated aq NaCl (10 mL) was added to quench the reaction. After removal of the volatile solvent under reduced pressure, the aqueous residue was extracted with CH_2Cl_2 (3 × 10 mL). The combined organic layer was dried over Na_2SO_4 and concentrated in vacuo, and the crude residue was directly used for the next step.

dx.doi.org/10.1021/jo3011792 | *J. Org. Chem.* 2013, 78, 1753−1759

The above crude residue was taken up in CH_2Cl_2 (5 mL), and to this solution were added DMAP (1.1 mg, 0.009 mmol) and Et_3N (0.06 mL, 0.431 mmol) with vigorous stirring under ice−water cooling bath. 2,4,6-Trichlorobenzoyl chloride (0.07 mL, 0.450 mmol) was then added in one portion. The reaction mixture was stirred at rt for 30 h and was then quenched with cold H_2O (10 mL) and extracted with CH_2Cl_2 (4 × 20 mL). The combined organic layers were dried over Na_2SO_4 and concentrated in vacuo. The crude residue was purified via silica gel column chromatography (gradient eluent: 10−30% EtOAc in hexane) to give the pure ester **12** (35.3 mg, 0.062 mmol, 42% over two steps) as a white solid.

12: R_f = 0.21 (30% EtOAc in hexane); $[\alpha]^{23}_D$ +29.9 (*c* 1.05, CH_2Cl_2); white solid; mp =176−177 °C; ^{1}H NMR (400 MHz, $CDCl_3$) δ 1.66 (s, 3H), 2.01−2.14 (m, 2H), 2.29 (dt, 1H, *J* = 8.4, 12.0 Hz), 2.56 (ddd, 1H, *J* = 2.4, 8.8, 12.0 Hz), 2.79 (dd, 1H, *J* = 8.8, 11.6 Hz), 3.35 (s, 3H), 3.37 (d, 1H, *J* = 7.2 Hz), 4.35 (br, 1H), 4.39 (t, 1H, *J* = 6.4 Hz), 4.84−4.89 (m, 2H); 4.95 (q, 1H, *J* = 7.2 Hz), 7.54 (d, 1H, *J* = 1.4 Hz), 7.52 (d, 1H, *J* = 1.4 Hz), 7.35−7.41 (m, 3H), 7.31 (s, 2H); ^{13}C NMR (100 MHz, $CDCl_3$) δ 26.8, 31.2, 33.7, 51.8, 52.3, 60.9, 63.7, 64.4, 72.0, 74.1, 82.2, 128.3, 129.1, 129.2, 131.7, 132.8, 135.2, 136.7, 159.3, 163.6, 169.8 (one carbon peak was missing due to overlapping); IR (thin film) cm^{-1} 2955 m, 1755s, 1579 m, 1373 m, 1265s, 1209 m, 1117 m, 734 m; mass spectrum (APCI) *m*/*e* (relative intensity) 574.0 (7) $(M + 6 + H)^+$, 572.1 (33) $(M + 4 + H)^+$, 569.2 (30) $(M + 2)^+$, 568.1 (96) $(M + H)^+$, 567.1 (90) $(M)^+$, 419.4 (9), 344.2 (22), 329.0 (85), 328.1 (21), 327.0 (100); HRMS (MALDI-TOF) *m*/*e* calcd for $C_{26}H_{24}Cl_3NO_7Na^+$ $(M + Na^+)$ 590.0516, found 590.0511.

Theoretical Calculations. Density functional theory calculations were performed using Gaussian 09.[10] Geometries were optimized in the gas phase using the B3LYP[11] functional, with a mixed basis set consisting of LANL2DZ on Zn and 6-31G(d) on all other atoms. The lowest-energy conformer of each species was identified through conformational searching. The B3LYP vibrational frequencies were used to characterize species as minima or transition states, and to obtain scaled[12] zero-point energies and thermal contributions to enthalpy and entropy. Single-point energies were then computed at the M06-2X/6-311+G(d,p) level[13] and used in conjunction with the B3LYP thermochemical corrections to obtain gas-phase activation enthalpies and free energies. Free energies of activation in dichloromethane were calculated by incorporating CPCM[14] solvation energies computed at the M06-2X/6-31G(d)-LANL2DZ level (UAKS radii). A standard state of 1 mol/L was used. Activation energies were also computed from single-point energy calculations at the B3LYP-D3[15] level, with zero-damping. The activation energies predicted by B3LYP and B3LYP-D3 for cycloadditions involving **3b** are provided in the Supporting Information, along with M06-2X activation energies for cycloadditions of **3c** with **4**−**7**.

■ ASSOCIATED CONTENT

Ⓢ Supporting Information

NMR spectra and characterizations for all new compounds, X-ray data (CIF) and thermal ellipsoid plots, optimized geometries and energies, computed barriers at the B3LYP and B3LYP-D3 levels for cycloadditions of **3b**, and M06-2X barriers for **3c**. This material is available free of charge via the Internet at http://pubs.acs.org.

■ AUTHOR INFORMATION

Corresponding Author

*E-mail: ekrenske@unimelb.edu.au, houk@chem.ucla.edu, rhsung@wisc.edu.

Notes

The authors declare no competing financial interest.

■ ACKNOWLEDGMENTS

We thank the NIH and Australian Research Council for generous financial support (GM-36700 to K.N.H., GM-66055 to R.P.H., and DP0985623 to E.H.K.), and the National Computational Infrastructure National Facility (Australia) and University of Melbourne for computer resources. E.H.K. also thanks the ARC Centre of Excellence for Free Radical Chemistry and Biotechnology for financial support. We thank Dr. Vic Young and Mr. Gregory T. Rohde of The University of Minnesota for X-ray crystallography.

■ REFERENCES

(1) For a key review on allenamide chemistry, see: Wei, L.-L.; Xiong, H.; Hsung, R. P. *Acc. Chem. Res.* **2003**, *36*, 773−782.

(2) For recent reviews on heteroatom-substituted oxyallyl intermediates, see: (a) Lohse, A. G.; Hsung, R. P. *Chem.—Eur. J.* **2011**, *17*, 3812−3822. (b) Harmata, M. *Chem. Commun.* **2010**, *46*, 8904−8922. (c) Harmata, M. *Recent Res. Devel. Org. Chem.* **1997**, *1*, 523−535.

(3) For general reviews on (4 + 3) cycloadditions, see: (a) Harmata, M. *Chem. Commun.* **2010**, *46*, 8886−8903. (b) Harmata, M. *Adv. Synth. Catal.* **2006**, *348*, 2297−2306. (c) Battiste, M. A.; Pelphrey, P. M.; Wright, D. L. *Chem.—Eur. J.* **2006**, *12*, 3438−3447. (d) Hartung, I. V.; Hoffmann, H. M. R. *Angew. Chem., Int. Ed.* **2004**, *43*, 1934−1949. (e) Rigby, J. H.; Pigge, F. C. *Org. React.* **2004**, 351−478. (f) Harmata, M.; Rashatasakhon, P. *Tetrahedron* **2003**, *59*, 2371−2395. (g) Harmata, M. *Acc. Chem. Res.* **2001**, *34*, 595−605. (h) Davies, H. M. L. In *Advances in Cycloaddition*; Harmata, M., Ed.; JAI: Stamford, CT, 1999; Vol. *5*, pp 119−164. (i) West, F. G. In *Advances in Cycloaddition*; Lautens, M., Ed.; JAI: Greenwich, CT, 1997; Vol. *4*, pp 1−40. (j) Harmata, M. *Tetrahedron* **1997**, *53*, 6235−6280. (k) Katritzky, A. R.; Dennis, N. *Chem. Rev.* **1989**, *89*, 827−861.

(4) For (4 + 3) cycloadditions of donor-substituted oxyallyls, including regioselective examples, see: (a) Föhlisch, B.; Krimmer, D.; Gehrlach, E.; Kaeshammer, D. *Chem. Ber.* **1988**, *121*, 1585−1594. (b) Murray, D. H.; Albizati, K. F. *Tetrahedron Lett.* **1990**, *31*, 4109−4112. (c) Walters, M. A.; Arcand, H. R.; Lawrie, D. J. *Tetrahedron Lett.* **1995**, *36*, 23−26. (d) Lee, J. C.; Jin, S.; Cha, J. K. *J. Org. Chem.* **1998**, *63*, 2804−2805. (e) Harmata, M.; Rashatasakhon, P. *Synlett* **2000**, 1419−1422. (f) Beck, H.; Stark, C. B. W.; Hoffmann, H. M. R. *Org. Lett.* **2000**, *2*, 883−886. (g) Myers, A. G.; Barbay, J. K. *Org. Lett.* **2001**, *3*, 425−428. (h) Harmata, M.; Ghosh, S. K.; Hong, X.; Wacharasindhu, S.; Kirchhoefer, P. *J. Am. Chem. Soc.* **2003**, *125*, 2058−2059. (i) MaGee, D. I.; Godineau, E.; Thornton, P. D.; Walters, M. A.; Sponholtz, D. J. *Eur. J. Org. Chem.* **2006**, 3667−3680. (j) Chung, W. K.; Lam, S. K.; Lo, B.; Liu, L. L.; Wong, W.-T.; Chiu, P. *J. Am. Chem. Soc.* **2009**, *131*, 4556−4557. (k) Lo, B.; Chiu, P. *Org. Lett.* **2011**, *13*, 864−867. (l) Liu, L. L.; Chiu, P. *Chem. Commun.* **2011**, *47*, 3416−3417.

(5) For our contributions to the field of (4 + 3) cycloadditions, see: (a) Xiong, H.; Hsung, R. P.; Berry, C. R.; Rameshkumar, C. *J. Am. Chem. Soc.* **2001**, *123*, 7174−7175. (b) Xiong, H.; Hsung, R. P.; Shen, L.; Hahn, J. M. *Tetrahedron Lett.* **2002**, *43*, 4449−4453. (c) Rameshkumar, C.; Xiong, H.; Tracey, M. R.; Berry, C. R.; Yao, L. J.; Hsung, R. P. *J. Org. Chem.* **2002**, *67*, 1339−1345. (d) Xiong, H.; Huang, J.; Ghosh, S. K.; Hsung, R. P. *J. Am. Chem. Soc.* **2003**, *125*, 12694−12695. (e) Rameshkumar, C.; Hsung, R. P. *Angew. Chem., Int. Ed.* **2004**, *43*, 615−618. (f) Huang, J.; Hsung, R. P. *J. Am. Chem. Soc.* **2005**, *127*, 50−51. (g) Antoline, J. E.; Hsung, R. P.; Huang, J.; Song, Z.; Li, G. *Org. Lett.* **2007**, *9*, 1275−1278. (h) Antoline, J. E.; Hsung, R. P. *Synlett* **2008**, 739−744. (i) Lohse, A. G.; Hsung, R. P.; Leider, M. D.; Ghosh, S. K. *J. Org. Chem.* **2011**, *76*, 3246−3257.

(6) (a) Krenske, E. H.; Houk, K. N.; Lohse, A. G.; Antoline, J. E.; Hsung, R. P. *Chem. Sci.* **2010**, *1*, 387−392. (b) Lohse, A. G.; Krenske, E. H.; Antoline, J. E.; Houk, K. N.; Hsung, R. P. *Org. Lett.* **2010**, *12*, 5506−5509. (c) Antoline, J. E.; Krenske, E. H.; Lohse, A. G.; Houk, K. N.; Hsung, R. P. *J. Am. Chem. Soc.* **2011**, *133*, 14443−14451.

(7) During the synthesis of ester **12** from cycloadduct **9**, an acyl transfer occurred during the esterification step.

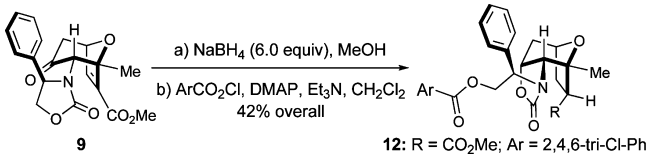

(8) (a) Wei, L.-L.; Hsung, R. P.; Xiong, H.; Mulder, J. A.; Nkansah, N. T. *Org. Lett.* **1999**, *1*, 2145−2148. (b) Berry, C. R.; Hsung, R. P.; Antoline, J. E.; Petersen, M. E.; Challeppan, R.; Nielson, J. A. *J. Org. Chem.* **2005**, *70*, 4038−4042.

(9) (a) Close, W. J. *J. Org. Chem.* **1950**, *15*, 1131−1134. (b) Roder, H.; Helmchen, G.; Peters, E.-M.; Peters, K.; von Schnering, H.-G. *Angew. Chem.* **1984**, *96*, 895−896.

(10) Frisch, M. J.; Trucks, G. W.; Schlegel, H. B.; Scuseria, G. E.; Robb, M. A.; Cheeseman, J. R.; Scalmani, G.; Barone, V.; Mennucci, B.; Petersson, G. A.; Nakatsuji, H.; Caricato, M.; Li, X.; Hratchian, H. P.; Izmaylov, A. F.; Bloino, J.; Zheng, G.; Sonnenberg, J. L.; Hada, M.; Ehara, M.; Toyota, K.; Fukuda, R.; Hasegawa, J.; Ishida, M.; Nakajima, T.; Honda, Y.; Kitao, O.; Nakai, H.; Vreven, T.; Montgomery, J. A., Jr.; Peralta, J. E.; Ogliaro, F.; Bearpark, M.; Heyd, J. J.; Brothers, E.; Kudin, K. N.; Staroverov, V. N.; Kobayashi, R.; Normand, J.; Raghavachari, K.; Rendell, A.; Burant, J. C.; Iyengar, S. S.; Tomasi, J.; Cossi, M.; Rega, N.; Millam, J. M.; Klene, M.; Knox, J. E.; Cross, J. B.; Bakken, V.; Adamo, C.; Jaramillo, J.; Gomperts, R.; Stratmann, R. E.; Yazyev, O.; Austin, A. J.; Cammi, R.; Pomelli, C.; Ochterski, J. W.; Martin, R. L.; Morokuma, K.; Zakrzewski, V. G.; Voth, G. A.; Salvador, P.; Dannenberg, J. J.; Dapprich, S.; Daniels, A. D.; Farkas, Ö.; Foresman, J. B.; Ortiz, J. V.; Cioslowski, J.; Fox, D. J. *Gaussian 09*, Revision A.02; Gaussian, Inc., Wallingford, CT, 2009.

(11) (a) Lee, C.; Yang, W.; Parr, R. G. *Phys. Rev. B* **1988**, *37*, 785−789. (b) Becke, A. D. *J. Chem. Phys.* **1993**, *98*, 1372−1377. (c) Becke, A. D. *J. Chem. Phys.* **1993**, *98*, 5648−5652.

(12) Merrick, J. P.; Moran, D.; Radom, L. *J. Phys. Chem. A* **2007**, *111*, 11683−11700.

(13) (a) Zhao, Y.; Truhlar, D. G. *Theor. Chem. Acc.* **2008**, *120*, 215−241. (b) Zhao, Y.; Truhlar, D. G. *Acc. Chem. Res.* **2008**, *41*, 157−167.

(14) (a) Barone, V.; Cossi, M. *J. Phys. Chem. A* **1998**, *102*, 1995−2001. (b) Cossi, M.; Rega, N.; Scalmani, G.; Barone, V. *J. Comput. Chem.* **2003**, *24*, 669−681.

(15) Grimme, S.; Antony, J.; Ehrlich, S.; Krieg, H. *J. Chem. Phys.* **2010**, *132*, 154104.

dx.doi.org/10.1021/jo3011792 | *J. Org. Chem.* 2013, 78, 1753−1759